

DETECTION OF MINING EXPLOSIONS FOR A SOUTHERN ASIA SEISMIC DATABASE

James M. Britton,¹ David B. Harris,² Ileana M. Tibuleac,¹ and Jessie L. Bonner¹

Weston Geophysical Corporation¹ and Lawrence Livermore National Laboratory²

Sponsored by National Nuclear Security Administration
Office of Nonproliferation Research and Engineering
Office of Defense Nuclear Nonproliferation

Contract No. DE-FG02-01-ER83341¹ and W-7405-ENG-48²

ABSTRACT

Weston Geophysical maintains a high-quality seismic research database for southern Asia consisting of detailed mining information together with seismograms recorded from mine blasts in India, Pakistan, Iran, and the surrounding regions. This digital mining database contains data on more than 240 mines and mineral deposits in southern Asia, including information on location, geology, commodities, production, mineralogy, references, operator, and mining explosion resources. The waveform data include seismograms from several stations in southern Asia including NIL, ABKT, HYB, and GBA, in addition to data from proprietary stations.

In the past year, we have employed different techniques to detect probable mining explosions. First, we have applied the waveform correlation method (Harris, 1991) to several months of data from each station of interest. Clusters of mining events were detected near stations in south and central India. Mining clusters were also detected near zinc mines in northwestern India. No mining clusters, however, were detected near station ABKT in southern Turkmenistan. An additional tool currently being developed to aid in the detection of mining events is a short-period Rayleigh wave (*Rg*) detector. Analysis of the waveform data was initiated employing a three-component detector to highlight *Rg* arrivals, which are often seen on mine-blast/shallow source, near-regional seismograms. The detector was modeled after the Chael (1997) automatic teleseismic Rayleigh-wave detection method; however we have modified the detector for regional distance and short-period (< 3 sec) applications. The modifications in the initial detection stage include: 1) application of a zero phase Butterworth filter between 0.4 and 1.3 Hz; 2) calculation of the covariance matrix for rotated waveforms; 3) estimation of the constants for the STA and LTA recursive filters; and 4) addition of two new weights of the detection function for planarity verification. We have observed that proper pre-filtering is essential for accuracy in back azimuth estimation. Therefore, once a detection has been declared, a Meyer Continuous Wavelet Transform at the estimated *Rg* frequency was applied as an alternative pre-filtering method, improving the backazimuth estimates. We have tested the detector on well-located clusters of mine events from central India.

Events detected by either of these two methods are located using single-station location techniques (Leidig *et al.*, 2003). We obtained satellite imagery for the areas covering the locations of the mining clusters. These images show the location of open-pit mines in close proximity (in most cases less than 10 km) from the centers of mining cluster epicenters. The imagery, event locations, station locations, and information on the mines are stored in an ArcView 8.3 geographic information system (GIS) database in which the digital seismic waveform data are linked. The database is updated as more mining clusters are detected and supplemental information (satellite imagery, mining information) is received.

OBJECTIVES

The objectives of this research are to catalog the mining resources of Iran, India, and Pakistan and to compile mine information together with mining explosion waveforms into a single, digital database.

RESEARCH ACCOMPLISHED

Mine Database

Continuous broadband waveform data have been obtained from the Incorporated Research Institutions for Seismology/International Deployment of Accelerometers (IRIS/IDA) stations ABKT, NIL, and PALK. The HYB waveforms were obtained from the Geoscope Network, and the GBA waveforms were obtained through the Atomic Weapons Exchange (AWE) in the United Kingdom. Table 1 shows the dates of some continuous data segments. Locations of these stations are shown in Figure 1, with proprietary stations indicated by P1 and P2 on the map and in this paper.

In addition to obtaining continuous waveform data at these stations, information on the mines and mining districts surrounding these stations is being compiled. Supplemental information, such as satellite imagery, is imported into the database to aid in determining ground truth for the locations of the detected mine blasts.

Table 1. Stations for which continuous data have been obtained

Station	Network	Dates	Segment Length [days]	Lat	Lon
ABKT	IRIS/IDA	4/9/02 – 10/22/02	196	37.9304	58.1189
NIL	IRIS/IDA	7/2/98 – 3/3/99	244	33.6500	73.2517
HYB	GEOSCOPE	4/21/99 – 5/20/99	30	17.4169	78.5531

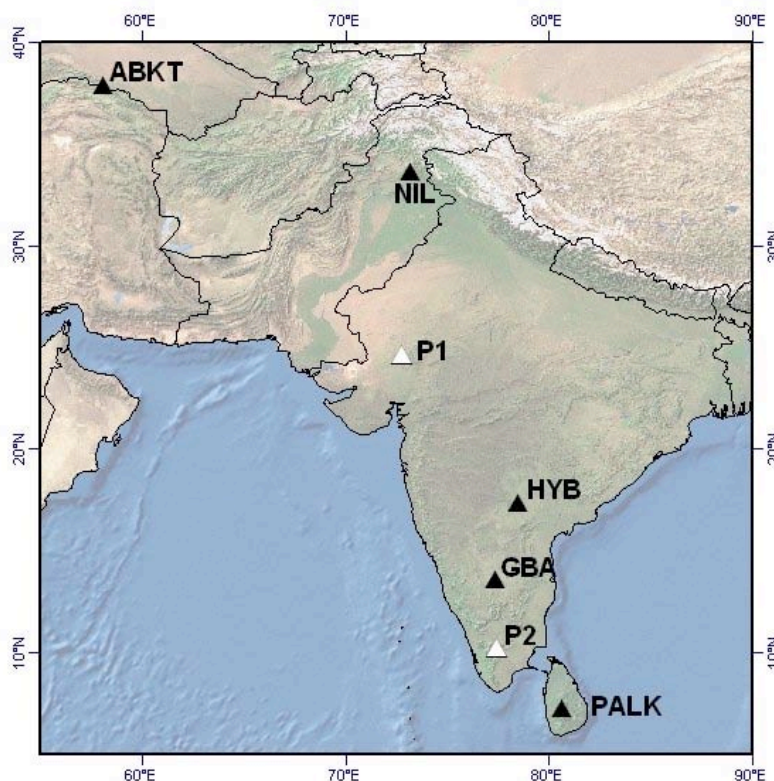


Figure 1. Location of IRIS/IDA stations, Geoscope station HYB, GBA, formerly operated by the Atomic Weapons Establishment (AWE) at Blacknest, and proprietary stations P1 and P2.

Detection of Mining Events from Continuous Data Using Waveform Correlation Techniques

Two methods for detecting mine blasts are employed in this research. The first is the waveform correlation method (Harris, 1991). This procedure involves the application of a simple STA/LTA detector to a month or more of continuous data. Detections are correlated to a certain threshold and assigned to clusters of events. Events in these clusters are examined by eye, and if the events appear to be mine blasts (based on the presence of the *R_g* phase or repeated occurrence during daylight hours) then the events in the cluster are located. The waveform correlation method has been the primary method for the detection of mine blasts in this research. This method has been used on data from HYB, ABKT, GBA, and the proprietary stations.

As an example of this application, a simple STA/LTA detector was applied to the first 40 days of continuous data from proprietary station P2 as an initialization for the waveform correlation. Two hundred and thirteen detections were made and the detected waveforms were correlated to a threshold of 0.4 into clusters of 2 or more events each. We developed subspace detectors for the two largest clusters, and these detectors were used to reprocess the entire P2 dataset for additional events in the two clusters.

Cluster 1, the largest cluster, contained 17 events upon initial inspection (33 events after further analysis). All of the events detected occurred between 1 April 2001 and 21 July 2001, with all but two events occurring between 1 April 2001 and 3 May 2001. The events occurred between 0500 and 0700 UTC (10:30 AM to 12:30 PM local time). Cluster 5, the second largest cluster, contained 11 events. These events occurred between the hours of 1000 and 1100 UTC (3:30 PM to 4:30 PM local time) from 5 April 2001 to 2 August 2001. Given the long durations of these sequences (111 days for Cluster 1; 119 days for Cluster 5) and the consistency of the origin times, the sources appear to be mines. Events from Cluster 5 also exhibit an *R_g* phases, which are consistent with shallow sources such as open-pit mine blasts. Figure 2 shows the locations of the clusters relative to P2 and nearby stations GBA and PALK. None of the events in either cluster were observed in the PALK dataset and no data from GBA are available after 1996. Figure 3 shows the detections, sorted by time of day, for a 4-month period.

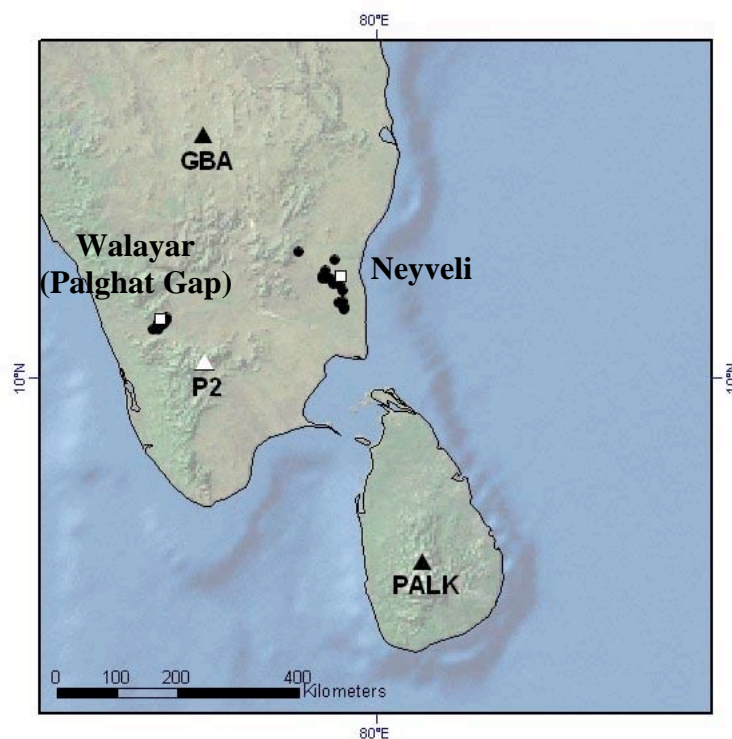


Figure 2. Location of the events from the two largest subspace detection clusters recorded at P2. Suspected mine blasts are plotted as dark circles. White squares represent locations of open-pit pits.

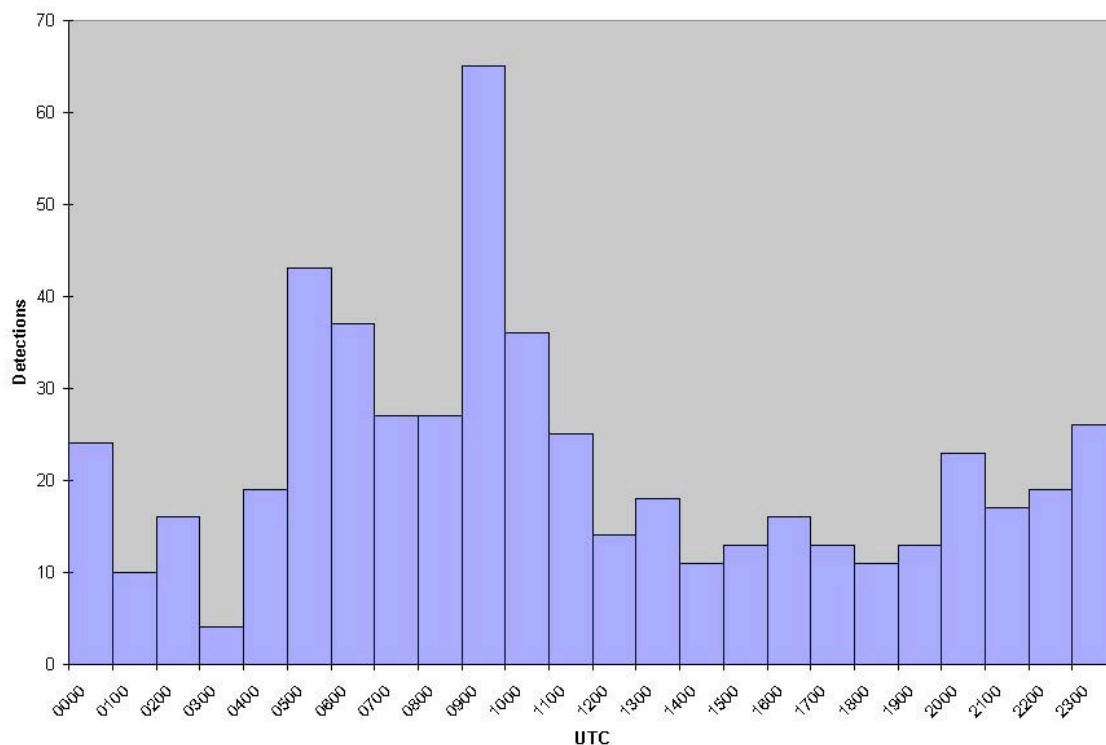


Figure 3. Event detections at station P2 between 29 March 2001 and 8 August 2001, sorted by time of day. Local time equals UTC plus 5.5 hours.

Detection of Possible Mining Events from Continuous Data using an Automated *R_g* Detector

The presence of *R_g* on waveforms indicates shallow source depth and, when detected repeatedly during daytime hours, it is often an indication of mining operations. Thus, the second method used to detect shallow events (possible mine blasts) is an automatic *R_g* detector. The *R_g* detector code has been tested on clusters of well-located events and we have developed routines necessary for automatic analysis of continuous data, as described below.

We modified the Chael (1997) detection method, which was developed for intermediate-period Rayleigh wave arrivals (17 to 22 sec), to account for the shorter periods (< 3 sec) characteristic of the *R_g* phase. The modifications included: 1) pre-filtering the waveforms between 0.4 and 1.3 Hz using a zero-phase, 3-pole Butterworth filter, 2) calculating the covariance matrix for rotated waveforms, 3) estimating the optimal constants for the STA and LTA recursive filters (Allen, 1982), and 4) using two additional weights of the detection function for planarity verification. The algorithm is coded in Matlab and will eventually be incorporated as a Matseis module (Young, 1997).

The *R_g* detector was applied to the data in two steps:

Step 1. Preliminary detection using Fourier techniques. First, the data was filtered between 0.4 – 1.3 Hz. Then, the algorithm was applied to the three components (Z, N, E) of the data in a moving time window with a step size of 0.5 seconds, over a swath of backazimuth ranging between 0 and 355 degrees. Detections were declared when the maximum value of the detection function was larger than an empirical threshold, which was calculated for each station.

Step 2. Back azimuth estimation. After detection was declared, values larger than 10% of the detection function's maximum value (see the lower plots in Figure 5) were plotted as a function of time and back azimuth. An initial back azimuth (bazF), corresponding to the largest values of the detection function, was estimated from the plot. All

the back azimuths in this study were calculated with a procedure described as the direction of the center of mass (Mardia, 1972), using the squared values of the detection function as weights.

We have observed that wavelet pre-filtering significantly improved the signal-to-noise ratio (SNR) of the R_g arrivals. Therefore, we decided to apply pre-filtering using a Meyer wavelet, once detection was declared, to assess whether it would improve the back azimuth estimates. The Meyer wavelet scale was calculated to correspond to the R_g period chosen by the analyst. A back azimuth was estimated for each R_g period. When using additional R_g periods (a total of three in this study), the final back azimuth (bazW) was calculated as the mean of the estimated back azimuths, using the SNR values for each scale as weights. We calculated SNR in the propagation plane as the ratio between the maximum amplitude and twice the standard deviation of the noise (Der and Shumway, 1999). We prefer this formula for SNR calculation to the classical ratio of six-second signal-to-noise rms because it accounts for the short duration (< 3 sec) of the R_g phase and for several seconds of possibly large S arrivals immediately preceding R_g .

The R_g detector was tested on 6 clusters (more than 60 events) recorded at stations in central and southern India. Unlike teleseismic Rayleigh waves, R_g has periods of less than 3 seconds. The frequency range of the Step 1 filter is very important for R_g detection and is specific to the event's epicentral distance. For the detector to be implemented for local and regional data processing, choosing the appropriate frequency range will be the key for successful detections.

Results for 24 central India events recorded at HYB are presented in Figure 4. These events belong to four clusters: 2, 10, 12 (GT20) and Cluster 9 (GT5).

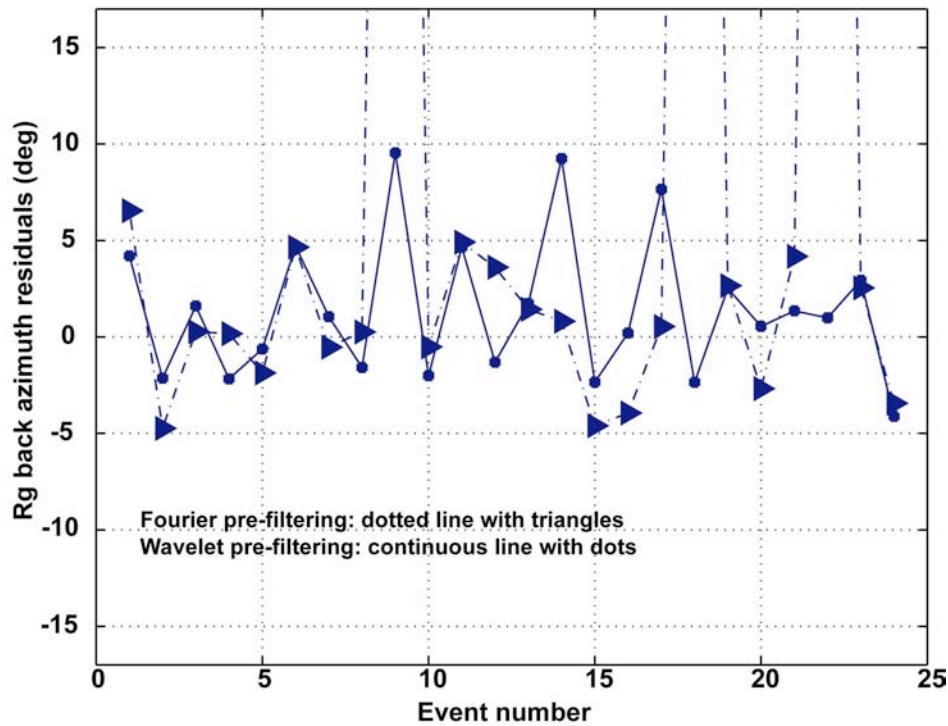


Figure 4. Back azimuth residuals estimated using Fourier pre-filtering (dotted line with triangles) and using wavelet pre-filtering (continuous line with dots). The residuals are relative to each cluster ground truth (GT) back azimuth. Events 1 and 2 are from Cluster 2, events 3 to 5 are from Cluster 9, events 6 to 9 are from Cluster 10 and events 10 to 24 are from Cluster 12.

Whereas R_g was detected as the most probable arrival in all 24 events using wavelet pre-filtering, it was detected as the most probable arrival in only 21 of 24 (87%) events using Fourier pre-filtering. Below we examine the three low SNR events that were not correctly detected using Fourier methods. For the event No. 18, 1999/11/29 09:39:03, from

Cluster 12, R_g is detected as one of three possible arrivals. The lower left plot of Figure 5 shows that the R_g arrival was detected with the correct backazimuth (40 degrees) at about 104 sec. However, the arrival that corresponds to the largest value of the detection function after Fourier pre-filtering was not the R_g . It was another Rayleigh-type arrival at ~ 107 sec, with a period of ~ 2.5 seconds and a back azimuth of 155 degrees (see Figure 4). In the right plots in Figure 5 we show that Meyer wavelet pre-filtering (scale 14, corresponding to 1.1 sec period) increased the R_g SNR dramatically.

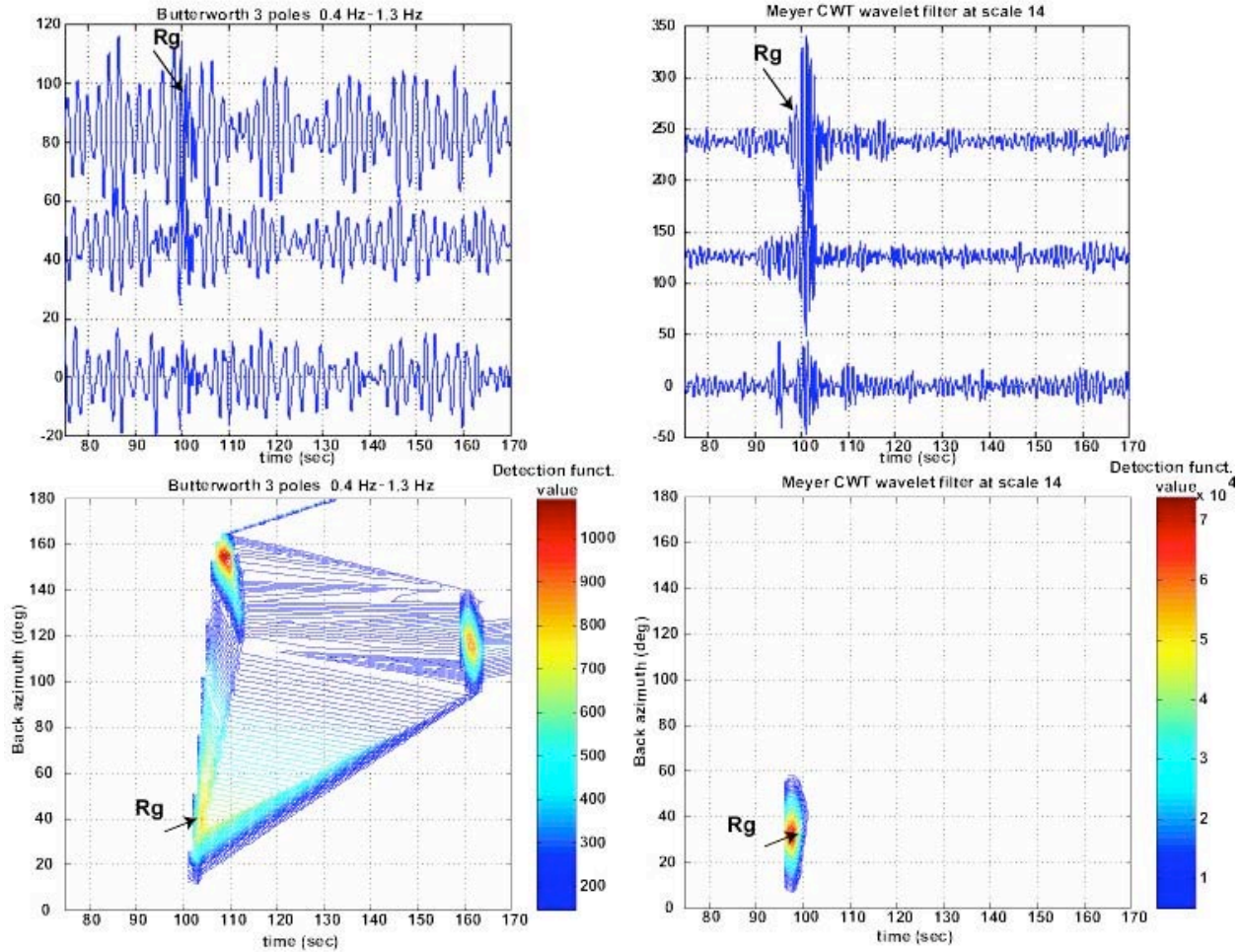


Figure 5. Top: Fourier and wavelet pre-filtered data of the 1999/11/29 09:39:03 event from Cluster 12, designated No. 18. Bottom: Detection function value as a function of time and back azimuth. As shown in the lower right plot, R_g is clearly detected in after wavelet pre-filtering. However, as shown in the lower left plot, R_g is only the third choice of the detector, based on the detection function value, after Fourier pre-filtering. The empirical detection threshold calculated for Fourier pre-filtering at HYB was 670.

The other two events not detected by Fourier pre-filtering were 9 and 22. For these two events the maximum of the detection function was below the empirical threshold value of 670 calculated at HYB. Wavelet pre-filtering improved the detection results for these events as well (see Figure 4).

The total estimated back azimuth sample standard deviation for the 24 events near HYB, using wavelet pre-filtering, was 3.7 degrees, equivalent to a maximum location error between 11 km (Clusters 2, 10, 12) and 12 km (Cluster 9). This result was better than the estimates using Fourier pre-filtering value and was comparable to the standard

deviation of the first arrival back azimuth residuals (3.8 degrees) calculated using data from a single station. Considering the location error (GT5 to GT20) for these 24 events, we consider the results encouraging. The R_g periods for this distance range were between 0.8 and 1.7 seconds.

Two clusters of events were analyzed at station P2. Cluster 1 (GT15) contained 33 events. Of these events, only one larger SNR event had a clear R_g arrival detected after data was Fourier pre-filtered between 0.6 and 4.5 Hz. No detections were found by the analyst, in several frequency intervals, for the other 32 events. For the one detected event, the GT back azimuth was 56.6 degrees and the first arrival back azimuth was estimated to be 67.1 degrees. Applying the R_g detector, we estimated the back azimuth as 66.2 degrees using Fourier pre-filtering and 59.9 degrees using wavelet pre-filtering. An empirical detection threshold of 650 was calculated for these events, for a frequency range of 0.4 – 1.3 Hz. Locations determined for the Cluster 1 events suggest the source is over 250 km northeast of the station. We attributed the strong attenuation of short period R_g from these events to the large event-station distance and to a propagation path with considerable topography.

Cluster 5 (GT2) contained 11 events located about 95 km distance from the station P2 at 317.2 degrees back azimuth. A frequency range of 0.6 – 4.5 Hz was used when searching for R_g in this cluster. Only four events, all detected, had visible R_g . The estimated back azimuth for the Fourier pre-filtering, as well as for the wavelet pre-filtering, differed by 30 degrees from the GT back azimuth for three of the events, and by 20 degrees for the fourth event. The largest first arrival back azimuth difference between events in this cluster was 13 degrees. There is considerable topography on the path from the station to the source for Cluster 5. Thus, the lack of R_g arrivals for this cluster suggests that either R_g is highly attenuated for this path or the events were too deep for R_g generation. However, the latter explanation is unlikely, as subsequent sections will show that the events are located very near open-pit mines as determined from satellite imagery. Further tests of the method are ongoing.

Our tests show that the R_g detector performs better when using wavelet pre-filtering and offers the advantage of improved back azimuth estimates. As wavelet decomposition considerably improves the performance of the detector, we will investigate using it as the primary pre-filtering mechanism. The R_g detector is currently being tested in automated mode and applied to continuous data from station HYB. Results from this analysis, as well as a comparison to the waveform correlation method, will be presented in the poster associated with this paper.

Location of Mining Events

During the past year, we have implemented SSLOC3D (Leidig *et al.*, 2003) to form single-station locations for the clusters determined from waveform correlation. SSLOC3D includes a polarization technique (Jurkevics, 1988) to determine back azimuths. A pilot study (Leidig *et al.*, 2003) showed that the polarization technique reduced the measurement error in determining back azimuths when compared to the three-component $f-k$ technique in Matseis (Young, 1997). SSLOC3D also estimates epicentral distances based on matching observed Lg - P times with travel time differences estimated using 3D velocity models. Prior to SSLOC3D implementation, we were using a single 1D P -wave velocity profile for central India to locate events at HYB, P1, and P2. The profile was based on the WINPAK3D P -wave velocities (Reiter *et al.*, 2001) beneath the HYB station. We determined that using the 3D P -wave travel-time grids, based on WINPAK3D, and an Lg travel-time grid based on a constant velocity of 3.6 km/sec could decrease the mislocation for most of the clusters in the database. The mislocations for P1 and HYB were decreased between 4 and 12 km through the use of SSLOC3D. An example of this improvement is shown in Figure 6, which compares 1D and SSLOC3D locations for mine events recorded at HYB. For SSLOC3D, 50% of the locations fall within the box drawn around the Ramagnundan mine complex as compared to none of the 1D locations. We do note that our mislocation errors for mines near P2 were slightly increased (< 3 km) using SSLOC3D as compared to 1D techniques. We note that these locations are model dependent and will improve as we develop better knowledge of the regional velocity structure.

Events from P2 Cluster 1 have been located near the large township of Neyveli in the southern Indian state of Tamil Nadu. Neyveli Lignite Corporation (NLC) Limited operates two open-cast mines (Mine I and Mine II) just south of Neyveli. The NLC website (<http://www.nlcindia.co.in/>) states that the mines are the largest mechanized lignite mines in India. Mine I and Mine II are located approximately 5 km apart. The mine locations were obtained from a map produced by Sinha and Sridharan (1999) in their noise level study of the Neyveli mines. Figure 7A shows the location of the Cluster 1 events relative to the township of Neyveli and the lignite mines. The orange cross in Figure 7A represents the average latitude and longitude of the cluster.

Cluster 5 events (Figure 7B) are centered near the town of Walayar in the state of Kerala near the Tamil Nadu border. Limestone mining is common in the Walayar area. Satellite imagery of the area has revealed two quarries, or open-pit mines, within 10 km of the centers of Cluster 5 and Cluster 3.

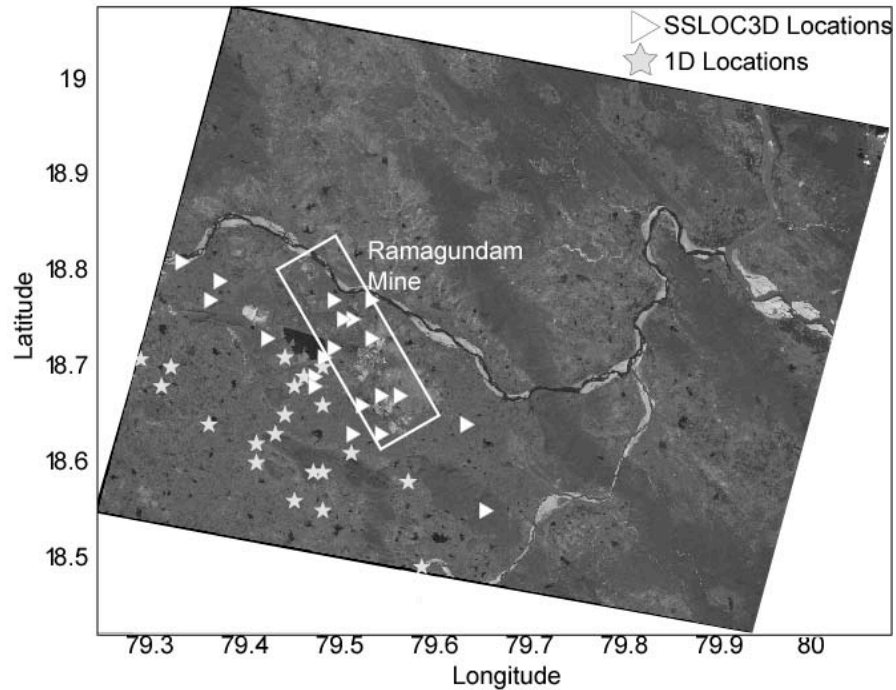


Figure 6. Epicenters determined from SSLOC3D (triangles) and 1D location techniques (stars) in relation to a large coal mining complex in central India.

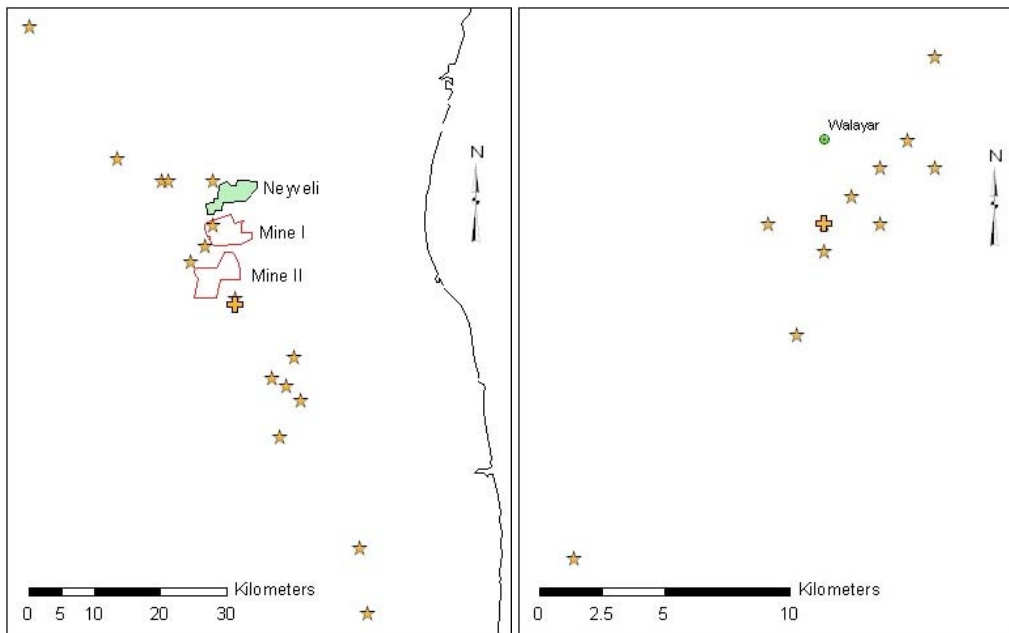


Figure 7. Single-station locations for suspected mine events. The figure on the left (Figure 7A) shows the events of Cluster 1. The figure on the right (Figure 7B) shows the events of Cluster 5. Centers of clusters are denoted by a cross.

CONCLUSIONS AND RECOMMENDATIONS

Information on mining activity around seismic stations in southern Asia is continually being compiled and updated. Continuous data for these stations have been analyzed by the waveform correlation method to detect events associated with nearby mines and mining districts. Waveform correlation has been the primary tool for detecting local mine blasts.

We have developed and tested a semi-automatic R_g detector. For 24 well-located events clustered near HYB, R_g is always detected after wavelet pre-filtering. Using Fourier pre-filtering between 0.4 and 1.3 Hz, R_g is detected as the most probable arrival for the 21 largest SNR events of the 24 (87%). The estimated R_g back azimuth sample standard deviation was 3.7 degrees, comparable to the standard deviation of the first arrival back azimuth residuals (3.8 degrees). Based on these results we will investigate the possibility of using wavelet pre-filtering in the initial detection stage instead of Fourier methods. For other events clustered near station P2, R_g was detected in all cases when it was visible on the seismogram. We plan to evaluate the detector on more GT data in India. Additionally, we are focused on making the whole procedure automatic. We consider the R_g detector tool a useful addition to the crosscorrelation method. The R_g detector offers the advantage of supplementary back azimuth estimates and therefore information on R_g propagation path characteristics, while the crosscorrelation method has the advantage of detecting mining events without visible R_g .

Detected waveforms from the clusters mentioned in this paper, along with other clusters detected in southern Asia by these techniques, are located using the SSLOC3D method (Leidig *et al.*, 2003). These waveforms are linked to an ArcView 8.3 geographic information system (GIS) database containing information on event location, satellite imagery, regional geology, station information, and mine information.

ACKNOWLEDGMENTS

We express our gratitude to Heather Hooper, Mark Leidig, and Delaine Reiter for their fruitful discussions and help on this project.

REFERENCES

- Allen, R. (1982), Automatic phase pickers: their present use and future prospects, *Bull. Seis. Soc. Am.*, **72**, S225-S242.
- Chael, E. P., (1997), An automated Rayleigh wave detection algorithm, *Bull. Seis. Soc. Am.*, 157-163.
- Der, Z. A. and R. H. Shumway, (1999), Phase onset time estimation at regional distances using the CUMSUM algorithm, *Phys. Earth Planet. Int.*, **113**, 227 –246.
- Harris, D.B. (1991). A waveform correlation method for identifying quarry explosions, *Bull. Seism. Soc. Am.*, **81**, 2395-2419.
- Jurkevics, A. (1988). Polarization analysis of three-component array data, *Bull. Seism. Soc. Am.*, **78**, 1725-1743.
- Leidig, M., D.T. Reiter, J. L. Bonner, and A. Rodgers, (in review). Applicability of 3D modeling techniques in creating single-station locations: a test case in southern Asia. Submitted to *Bull. Seism. Soc. Am.*
- Mardia, K. V. (1972), Statistics of directional data, Academic Press, New York
- Reiter, D. T., M. Johnson, A. Rosca, C. Vincent, (2001). Development of a regional 3D velocity model of the Pakistan region for improved seismic event location. Final Report, Weston Geophysical, 27 p.
- Sinha, S. and P.V. Sridharan (1999). Present and future assessment of noise level in the Neyveli region, *Journal of Environmental Studies and Policy*, 2(1): 1-13.
- Young, C., (1997). Matseis: a seismic toolbox for MATLAB, *Proceedings of the 18th Annual DoD/DOE Seismic Research Symposium*.